Cascades, thermalization, and eddy viscosity in helical Galerkin truncated Euler flows

G. Krstulovic,[1] P. D. Mininni,[2,3] M. E. Brachet,[1,3] and A. Pouquet[3]
[1]*Laboratoire de Physique Statistique de l'Ecole Normale Supérieure, associé au CNRS et aux Universités Paris VI et VII, 24 Rue Lhomond, 75231 Paris, France*
[2]*Departamento de Física, Facultad de Ciencias Exactas y Naturales, Universidad de Buenos Aires, Ciudad Universitaria, 1428 Buenos Aires, Argentina*
[3]*NCAR, P.O. Box 3000, Boulder, Colorado 80307-3000, USA*
(Received 4 June 2008; revised manuscript received 23 February 2009; published 6 May 2009)

The dynamics of the truncated Euler equations with helical initial conditions are studied. Transient energy and helicity cascades leading to Kraichnan helical absolute equilibrium at small scales, including a linear scaling of the relative helicity spectrum are obtained. Strong helicity effects are found using initial data concentrated at high wave numbers. Using low-wave-number initial conditions, the results of Cichowlas *et al.* [Phys. Rev. Lett. **95**, 264502 (2005)] are extended to helical flows. Similarities between the turbulent transient evolution of the ideal (time-reversible) system and viscous helical flows are found. Using an argument in the manner of Frisch *et al.* [Phys. Rev. Lett. **101**, 144501 (2008)], the excess of relative helicity found at small scales in the viscous run is related to the thermalization of the ideal flow. The observed differences in the behavior of truncated Euler and (constant viscosity) Navier-Stokes are qualitatively understood using the concept of eddy viscosity. The large scales of truncated Euler equations are then shown to follow quantitatively an effective Navier-Stokes dynamics based on a variable (scale dependent) eddy viscosity.

DOI: 10.1103/PhysRevE.79.056304 PACS number(s): 47.27.Gs, 05.20.Jj

I. INTRODUCTION

The role played by helicity in turbulent flows is not completely understood. Helicity is relevant in many atmospheric processes, such as rotating convective (supercell) thunderstorms, the predictability of which may be enhanced because of its presence [1]. However helicity, which is a conserved quantity in the three-dimensional (3D) Euler equation, plays no role in the original theory of turbulence of Kolmogorov. Later studies of absolute equilibrium ensembles for truncated helical Euler flows by Kraichnan [2] gave support to a scenario where in helical turbulent flows both the energy and the helicity cascade toward small scales [3], a phenomena recently verified in numerical simulations [4–6]. The thermalization dynamics of nonhelical spectrally truncated Euler flows were studied in [7]. Long-lasting transients due to the effect of thermalized small-scales were shown to behave similarly to the dissipative Navier-Stokes (NS) equation. Note that analogous dissipative mechanisms involving small-scale thermalization were proposed in the contexts of lattice gases and superfluidity. The thermalizing quantities are respectively discrete Boolean entities [8] in lattice gases [9] and sound waves in superfluid turbulence [10]. Also note that the Galerkin truncated nonhelical Euler dynamics was recently found to emerge as the asymptotic limit of high-order hyperviscous hydrodynamics and that bottlenecks observed in viscous turbulence may be interpreted as an incomplete thermalization [11].

In this paper we study truncated helical Euler flows and consider the transient turbulent behavior as well as the late time equilibrium of the system. Here is a short summary of our main results. The relaxation toward a Kraichnan helical absolute equilibrium [2] is observed for the first time. Transient mixed energy and helicity cascades are found to take place, while more and more modes gather into the Kraichnan time-dependent statistical equilibrium. The results obtained in [7] for nonhelical flows are extended to the helical case. Strong helicity effects are also found using initial data concentrated at high wave numbers. The concept of eddy viscosity, as previously developed in [7,12], is used to qualitatively explain differences observed between the truncated Euler and high-Reynolds number (fixed viscosity) Navier-Stokes. Finally, the truncated Euler large scale modes are shown to quantitatively follow an effective Navier-Stokes dynamics based on a (time and wave-number dependents) eddy viscosity that does not depend explicitly on the helicity content in the flow.

II. METHODS

Performing spherical Galerkin truncation at wave-number $k_{\max}$ on the incompressible ($\nabla\cdot\mathbf{u}=0$) and spatially periodic Euler equation $\partial_t\mathbf{u}+(\mathbf{u}\cdot\nabla)\mathbf{u}=-\nabla p$ yields the following finite system of ordinary differential equations for the Fourier transform of the velocity $\hat{\mathbf{u}}(\mathbf{k})$ ($\mathbf{k}$ is a 3D vector of relative integers satisfying $|\mathbf{k}|\leq k_{\max}$):

$$\partial_t\hat{u}_\alpha(\mathbf{k},t)=-\frac{i}{2}\mathcal{P}_{\alpha\beta\gamma}(\mathbf{k})\sum_{\mathbf{p}}\hat{u}_\beta(\mathbf{p},t)\hat{u}_\gamma(\mathbf{k}-\mathbf{p},t), \qquad (1)$$

where $\mathcal{P}_{\alpha\beta\gamma}=k_\beta P_{\alpha\gamma}+k_\gamma P_{\alpha\beta}$ with $P_{\alpha\beta}=\delta_{\alpha\beta}-k_\alpha k_\beta/k^2$.

This time-reversible system exactly conserves the energy $E=\Sigma_k E(k,t)$ and helicity $H=\Sigma_k H(k,t)$, where the energy and helicity spectra $E(k,t)$ and $H(k,t)$ are defined by averaging, respectively $\frac{1}{2}|\hat{\mathbf{u}}(\mathbf{k}',t)|^2$, and $\hat{\mathbf{u}}(\mathbf{k}',t)\cdot\hat{\omega}(-\mathbf{k}',t)$ ($\omega=\nabla\times\mathbf{u}$ is the vorticity) on spherical shells of width $\Delta k=1$. It is trivial to show from the definition of vorticity that $|H(k,t)|\leq 2kE(k,t)$.

We will use as initial condition $\mathbf{u}_0$ the sum of the two Arnold, Beltrami, and Childress (ABC) flows in the modes $k=3$ and $k=4$,

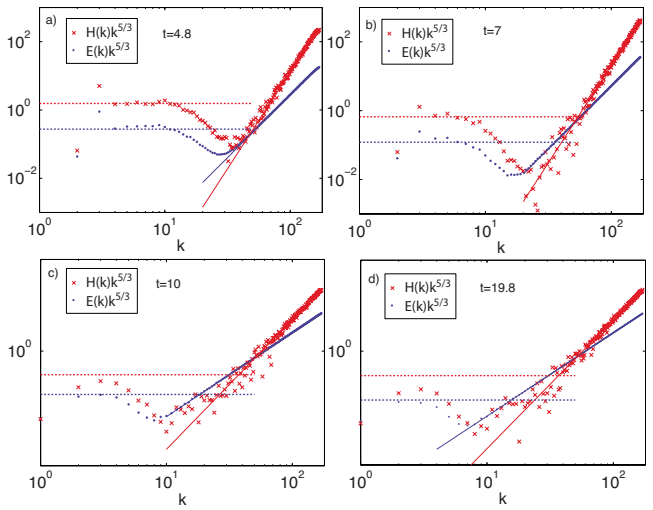

FIG. 1. (Color online) Compensated energy (•••) and helicity spectra (×××) with the predictions [Eq. (4))] in solid lines and Eq. (6) in dotted lines. (a) $t=4.8$. (b) $t=7$. (c) $t=10$. (d) $t=19.8$.

$$\mathbf{u}_0(x,y,z) = \mathbf{u}^{(3)}_{\mathrm{ABC}}(x,y,z) + \mathbf{u}^{(4)}_{\mathrm{ABC}}(x,y,z), \tag{2}$$

where the basic ABC flow is a maximal helicity stationary solution of Euler equations in which the vorticity is parallel to the velocity, explicitly given by

$$\mathbf{u}^{(k)}_{\mathrm{ABC}}(x,y,z) = \frac{u_0}{k^2}\{[B\cos(ky) + C\sin(kz)]\hat{x} + [C\cos(kz) + A\sin(kx)]\hat{y} + [A\cos(kx) + B\sin(ky)]\hat{z}\}. \tag{3}$$

The parameters will be set to $A=0.9$, $B=1$, $C=1.1$, and $u_0 = (A^2+B^2+C^2)^{-1/2}(1/3^4+1/4^4)^{-1/2}$. With this choice of normalization the initial energy is $E=0.5$ and helicity $H=3\times4\times(3^3+4^3)/(3^4+4^4)=3.24$.

Numerical solutions of Eq. (1) are efficiently produced using a pseudospectral general-periodic code [13] with 512^3 Fourier modes that is dealiased using the 2/3 rule [14] by spherical Galerkin truncation at $k_{\max}=170$. The equations are evolved in time using a second-order Runge-Kutta method, and the code is fully parallelized with the message passing interface (MPI) library. The numerical method used is nondispersive and conserves energy and helicity with high accuracy.

III. SIMULATIONS

Figure 1 shows the time evolution of the energy and helicity spectra that evolve from Eq. (2) compensated by $k^{5/3}$. The plots clearly display a progressive thermalization similar to that obtained in Cichowlas *et al.* [7] but with the nonzero helicity cascading to the right.

The truncated Euler equation dynamics is expected to reach at large times an absolute equilibrium that is a statistically stationary Gaussian exact solution of the associated Liouville equation [15,16]. When the flow has a nonvanishing helicity, the absolute equilibria of the kinetic energy and helicity predicted by Kraichnan [2] are

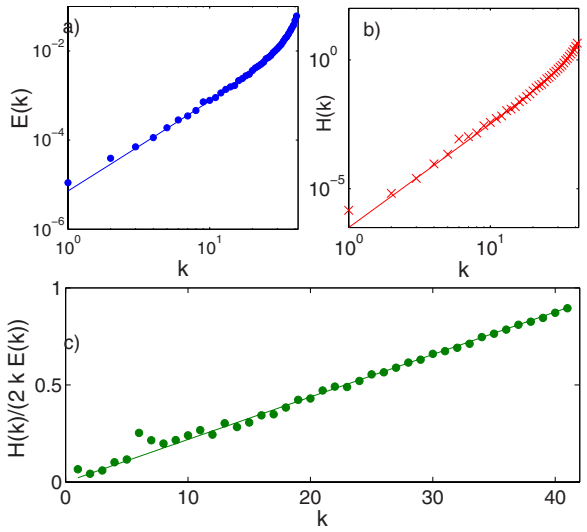

FIG. 2. (Color online) Thermalized energy at $t=21$ for a run with (a) $k_{\max}=42$, (b) helicity, and (c) relative helicity spectra with the predictions [Eq. (4)] (solid lines) corresponding to initial condition (2) but with wave numbers [3,4] changed to [28, 30].

$$E(k) = \frac{k^2}{\alpha}\frac{4\pi}{1-\beta^2k^2/\alpha^2}, \quad H(k) = \frac{k^4\beta}{\alpha^2}\frac{8\pi}{1-\beta^2k^2/\alpha^2}, \tag{4}$$

where $\alpha>0$ and $\beta k_{\max}<\alpha$ to ensure integrability. The values of α and β are uniquely determined by the total amount of energy and helicity (verifying $|H|\le 2k_{\max}E$) contained in the wave-number range $[1,k_{\max}]$ [2].

The final values of α and β (when total thermalization is obtained) corresponding to the initial energy and helicity are $\alpha=4.12\times10^7$ and $\beta=7695$. Therefore the dimensionless number β^2k^2/α^2 is at most of the order 10^{-4} and Eq. (4) thus lead to almost pure power laws for the energy and helicity spectra, as is manifested in Fig. 1(d). Figure 1 thus shows a time evolving helical quasiequilibrium. The Kraichnan prediction [Eq. (4)] for the high-k part of the spectra are shown (in solid lines) in Fig. 1. The plot shows an excellent agreement with the prediction.

To obtain stronger helicity effects requires a different type of initial data. Modifying in the initial condition [Eq. (2)] the wave numbers [3,4] to [28,30] and running with $k_{\max}=42$ yields $\beta^2k_{\max}^2/\alpha^2=0.846$. The final energy, helicity, and relative helicity spectra are displayed in Fig. 2, where strong helicity effects are apparent. The results are again consistent with the prediction given by Eq. (4). However note that these strong effects were obtained using initial data with $k_0 \sim k_{\max}$ that precludes the cascading of the initial energy and helicity to much higher wave numbers.

IV. THERMALIZED ENERGY AND HELICITY

In order to study the thermalization dynamics of the main run presented in Fig. 1 in the spirit of Cichowlas *et al.* [7], we define $k_{\mathrm{th}}(t)$ as the wave number where the thermalized power-law zone starts. We define the thermalized energy and helicity as

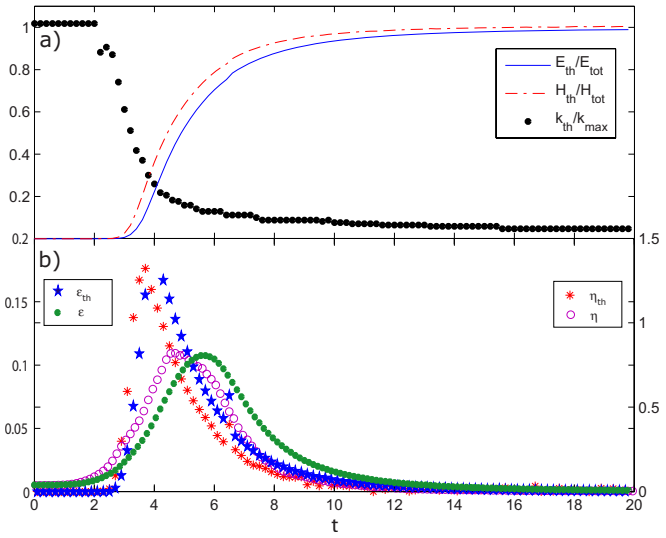

FIG. 3. (Color online) (a) Temporal evolution of $E_{\rm th}$ (–), $H_{\rm th}$ (–·–), and $k_{\rm th}(t)$ (···) normalized by their respective initial values. $E_{\rm tot}=0.5$, $H_{\rm tot}=3.24$, and $k_{\rm max}=170$. (b) Left vertical axis: temporal evolution of $\epsilon_{\rm th}=\frac{dE_{\rm th}}{dt}$ (★★★) and Navier-Stokes energy dissipation $\epsilon=2\nu_0\Sigma_{k=1}^{k_{\rm max}}k^2E(k)$ (•••). Right vertical axis: $\eta_{\rm th}=\frac{dH_{\rm th}}{dt}$ (∗∗∗) and NS helicity dissipation $\eta=\nu_0\Sigma_{k=1}^{k_{\rm max}}k^2H(k)$ (◦◦◦).

$$E_{\rm th}(t)=\sum_{k_{\rm th}(t)}^{k_{\rm max}}E(k,t),\quad H_{\rm th}(t)=\sum_{k_{\rm th}(t)}^{k_{\rm max}}H(k,t),\tag{5}$$

where $E(k,t)$ and $H(t,k)$ are the energy and helicity spectra.

The temporal evolutions of $E_{\rm th}, H_{\rm th}$, and $k_{\rm th}(t)$ are shown in Fig. 3. The values of $\alpha(t)$ and $\beta(t)$ during thermalization can then be obtained from $E_{\rm th}(t)$, $H_{\rm th}(t)$, and $k_{\rm th}(t)$ by inverting the system of Eqs. (5) using $\frac{\beta^2}{\alpha^2}k_{\rm max}^2\ll 1$.

Figures 1 and 3 clearly display a progressive thermalization similar to that obtained in Cichowlas *et al.* [7] but with the nonzero helicity cascading to the right. The low-k part of the compensated spectrum in Fig. 1 presents a flat zone that amounts to $k^{-5/3}$ scaling for both the energy and helicity spectra. This $k^{-5/3}$ behavior was predicted by Brissaud *et al.* [3] in viscous fluids when there are simultaneous energy and helicity cascades. The energy and helicity fluxes, ϵ and η, respectively, determine the prefactor in the inertial range of the spectra:

$$E(k)\sim\epsilon^{2/3}k^{-5/3},\quad H(k)\sim\eta\epsilon^{-1/3}k^{-5/3}.\tag{6}$$

Helical flows have been also studied in high-Reynolds number numerical simulations of the NS equation. Simultaneous energy and helicity cascades leading to the scaling [Eq. (6)] have been confirmed when the system is forced at large scales [4–6].

The energy and helicity fluxes, ϵ and η, at intermediate scales in our truncated Euler simulation can be estimated using the time derivative of the thermalized energy and helicity: $\epsilon_{\rm th}=\frac{dE_{\rm th}}{dt}$ and $\eta_{\rm th}=\frac{dH_{\rm th}}{dt}$, whose temporal evolutions are shown in Fig. 3. The predictions [Eq. (6)] for the low-k part of the spectra are shown (in dotted lines) in Fig. 1. The plot shows a good agreement with the data. Note that Fig. 1(a) corresponds to $t=4.8$ that is just after the time when both the maximum energy and helicity fluxes (to be interpreted below as "dissipation" rates of the nonthermalized components of the energy and the helicity) are achieved, see Fig. 3. In this way $E_{\rm th}$ and $H_{\rm th}$ determine the thermalized part of the spectra, while their time derivative determines an inertial range.

V. DISSIPATION AND TRUNCATED EULER

We now compare the dynamics of the truncated Euler equation with that of the unforced high-Reynolds number NS equation [i.e., Eq. (1) with $-\nu_0k^2\hat{u}_\alpha(\mathbf{k},t)$ added in the right-hand side] using initial condition (2). The viscosity is set to $\nu_0=5\times10^{-4}$, the smallest value compatible with accurate computations using $k_{\rm max}=170$. A behavior qualitatively similar to that of the truncated Euler equation is obtained [see Fig. 3(b)]. However, the maxima of the energy and helicity fluxes (or dissipation rates) occur later and with smaller values.

We referred above to dissipation in the context of the ideal (time-reversible) flow. A proper definition of dissipation in the truncated Euler flow is now in order. Thermalized modes in truncated Euler are known to provide an eddy viscosity $\nu_{\rm eddy}$ to the modes with wave numbers below the transition wave number [7]. It was shown in [12] that Monte Carlo determinations of $\nu_{\rm eddy}$ are given with good accuracy by the Eddy damped quasinormal Markovian (EDQNM) two-point closure, previously known to reproduce well direct numerical simulation results [17]. For helical flows, the EDQNM theory provides coupled equations for the energy and helicity spectra [18], in which using Eq. (4) in an analogous way to [12] we find a very small correction of $\nu_{\rm eddy}$ that depends on the total amount of helicity and is of order $\Delta\nu_{\rm eddy}/\nu_{\rm eddy}\sim\beta k_{\rm max}/\alpha\sim10^{-2}$. Thus the presence of helicity does not affect significantly the dissipation at large scales and can be safely neglected in the eddy viscosity expressions. Similar results are found in a large-eddy simulation approach to Navier-Stokes dynamics: the adjunction of helical contributions to eddy viscosity was not producing significant changes in the results [19] (note however that such is not the case in the presence of rotation [20]).

The eddy viscosity has a strong dependence in k and can also be obtained, in the limit $k/k_{\rm max}\to0$, from the EDQNM eddy viscosity of Lesieur and Schertzer [21] using here an energy spectrum $E(k)\sim k^2$. The result reads as

$$\nu_{\rm eddy}=\frac{\sqrt{E_{\rm th}}}{k_{\rm max}}\frac{7}{\sqrt{15\lambda}},\tag{7}$$

with $\lambda=0.36$ (the one parameter of the EDQNM approach, chosen as to recover a Kolmogorov constant as measured in the laboratory). The eddy viscosity $\nu_{\rm eddy}$ is thus an increasing function of time, see $E_{\rm th}(t)$ in Fig. 3.

The time evolution of truncated Euler and Navier-Stokes spectra are compared in Fig. 4. At early times the value of $E_{\rm th}$ is very small and therefore the NS viscosity ν_0 is larger than $\nu_{\rm eddy}$, as manifested by the NS dissipative zone in Fig. 4(a). As $E_{\rm th}(t)$ increases, both viscosities become equal ($t=2.7$). Later, at $t=3.8$, the Navier-Stokes spectrum crosses

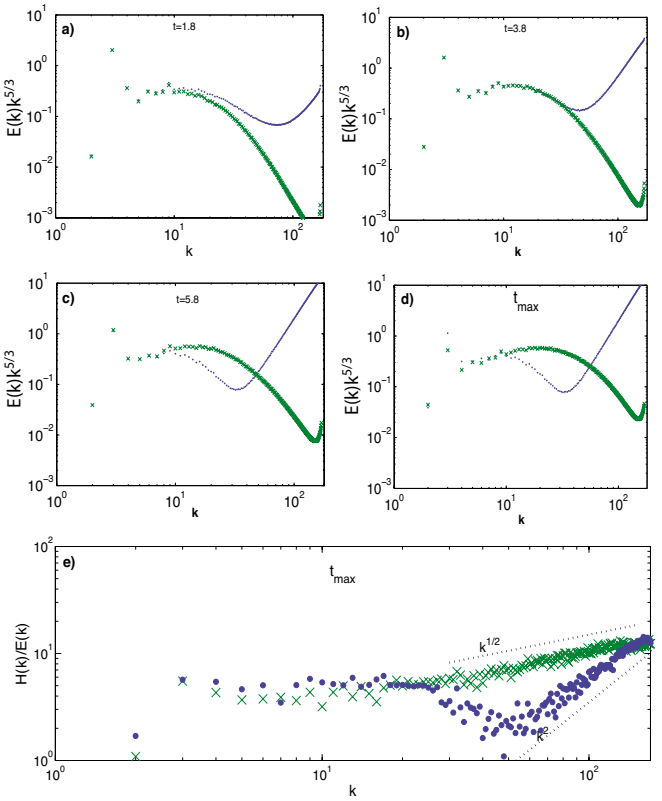

FIG. 4. (Color online) Compensated energy spectra $k^{5/3}E(k)$ of truncated Euler (···) and Navier-Stokes (×××). (a) $t=1.8$, (b) $t=3.8$, (c) $t=5.8$. (d) Maximum energy-dissipation time ($t=4.4$ for truncated Euler and $t=5.6$ for NS). (e) Compensated relative helicity spectra $H(k)/E(k)$ of truncated Euler (···) and Navier-Stokes (×××) at maximum energy-dissipation time. The dashed black lines show $k^{1/2}$ and k^2 power laws.

the truncated Euler one [Fig. 4(b)]. The eddy viscosity ν_{eddy} is then much larger than ν_0 and the truncated Euler dissipative zone lies below the NS one, see Fig. 4(c). This behavior is also conspicuous when the spectra are compared at maximum energy-dissipation time ($t=4.4$ for truncated Euler and $t=5.6$ for NS), see Fig. 4(d). The corresponding relative helicity spectra $H(k)/[2kE(k)]$, compensated by $2k$, is displayed in Fig. 4(d). A flat compensated spectrum in Fig. 4(d) is apparent throughout the inertial range (up to $k\sim 25$) for both the NS and the truncated Euler runs. This amounts to a scaling of k^{-1} for the relative helicity, corresponding to the previously discussed approximate $k^{-5/3}$ law for both the energy and helicity spectra. As Kraichnan predicted, in the thermalized range of the truncated Euler run the compensated spectrum of relative helicity goes as k^2. At small scales the NS compensated spectrum of relative helicity grows, possibly as $k^{1/2}$ or steeper, indicating, as previously noted (see Fig. 16 of Ref. [6]), that the spectrum of helicity at small scales is dropping slower than the spectrum of energy.

The decay of relative helicity in the inertial range can be interpreted as a recovery of mirror symmetry in the small scales. However, in the thermalized range of the truncated Euler run, the smallest scales have maximum helicity. These two results taken together, along with the arguments of Frisch *et al.* [11] relating bottlenecks to incomplete thermalization, strongly suggest that the excess of relative helicity observed at small scales in viscous runs [the $k^{1/2}$ law of Fig. 4(d)] is related to the phenomenon of thermalization in the ideal runs.

The different time scales of behavior of the truncated Euler and Navier-Stokes runs apparent in Figs. 3 and 4 were qualitatively explained above in terms of the time dependence of ν_{eddy}. We now proceed to check more quantitatively the validity of an effective dissipation description of thermalization in truncated Euler. To wit, we introduce an effective Navier-Stokes equation for which the dissipation is produced by an effective viscosity that depends on time and wave number.

We will use the effective viscosity obtained in [12] which is consistent with both direct Monte Carlo calculations and EDQNM closure and is explicitly given by

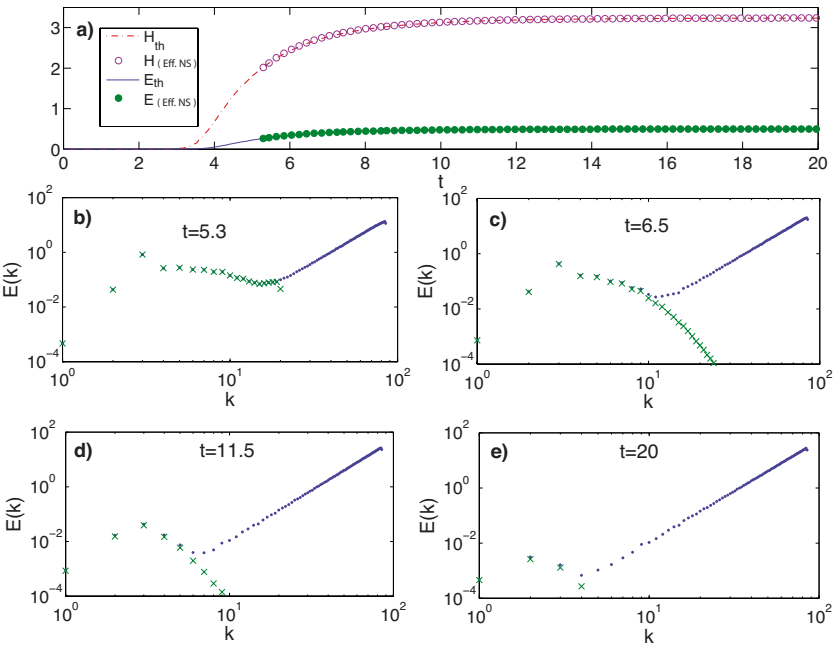

FIG. 5. (Color online) Effective NS run with $k_{\max}=85$. (a) Temporal evolution of E_{th} (–), H_{th} (·–·) from truncated Euler, energy (•••), and helicity (◦◦◦) from effective NS. [(b)–(e)] Temporal evolution of compensated energy spectra of truncated Euler (···) and effective Navier-Stokes (×××).

$$\nu_{\text{eff}}(k) = \nu_{\text{eddy}} e^{-3.97k/k_{\max}},$$

with ν_{eddy} given in Eq. (7).

We thus integrate Eq. (1) with the viscous term $-\nu_{\text{eff}}(k)k^2\hat{u}_\alpha(\mathbf{k},t)$ added to the right-hand side. The parameter E_{th} that fixes the eddy viscosity in Eq. (7) is evolved using the effective NS dissipation by

$$\frac{dE_{\text{th}}}{dt} = \sum_{k=1}^{k_{\max}} 2\nu_{\text{eff}}(k)k^2E(k). \tag{8}$$

This ensures consistency between the effective NS dissipated energy and the truncated Euler thermalized energy that drives ν_{eddy}.

To initialize the effective NS equation we integrate the truncated Euler Eq. (1) with initial condition (2) until the k^2-thermalized zone is clearly present ($t=4.77$). The value of E_{th} is then computed using Eq. (5). The low-passed velocity $\mathbf{u}^<$, defined by

$$\mathbf{u}^<(\mathbf{r}) = \sum \frac{1}{2}\{1+\tanh[2(|\mathbf{k}|-k_{\text{th}})]\}\hat{\mathbf{u}}_\mathbf{k}e^{i\mathbf{k}\cdot\mathbf{r}},$$

is used as initial data for the effective Navier-Stokes dynamics.

Results of a truncated Euler and effective NS with $k_{\max}=85$ are shown in Fig. 5. In Fig. 5(a) the energy and helicity dissipated in effective NS [$E_{\text{tot}}-E(t)$ and $H_{\text{tot}}-H(t)$, respectively] are compared to E_{th} and H_{th} showing a good agreement. Next, the temporal evolution of both energy spectra from the initial time $t=5.3$ [Fig. 5(b)] to $t=20$ [Fig. 5(e)] is confronted, demonstrating that the low-k dynamics of truncated Euler is well reproduce by the effective Navier-Stokes equations.

VI. CONCLUSION

In summary, we observed the relaxation of the truncated Euler dynamics toward a Kraichnan helical absolute equilibrium. Strong helicity effects were found using initial data concentrated at high wave numbers. Using low-wave-number initial conditions, transient mixed energy, and helicity cascades were found to take place. Eddy viscosity was found to qualitatively explain the different behaviors of truncated Euler and (constant viscosity) Navier-Stokes. The excess of relative helicity at small scales in the viscous run was related to the thermalization in the ideal runs, using an argument in the manner of Frisch *et al.* [11]. The large scale of the Galerkin truncated Euler were shown to quantitatively follow an effective Navier-Stokes dynamics based on a variable helicity-independent eddy viscosity. As a result, with its built-in eddy viscosity, the Galerkin truncated Euler equations appears as a minimal model of turbulence.

ACKNOWLEDGMENTS

We acknowledge discussions with U. Frisch and J. Z. Zhu. P.D.M. acknowledges support from the Carrera del Investigador Científico of CONICET. The computations were carried out at NCAR and IDRIS (CNRS). NCAR was sponsored by NSF. G.K. acknowledges the support of CONICYT.

[1] D. K. Lilly, J. Atmos. Sci. **43**, 126 (1986).
[2] R. H. Kraichnan, J. Fluid Mech. **59**, 745 (1973).
[3] A. Brissaud, U. Frisch, J. Leorat, M. Lesieur, and A. Mazure, Phys. Fluids **16**, 1366 (1973).
[4] V. Borue and S. A. Orszag, Phys. Rev. E **55**, 7005 (1997).
[5] Q. N. Chen, S. Y. Chen, and G. L. Eyink, Phys. Fluids **15**, 361 (2003).
[6] P. D. Mininni, A. Alexakis, and A. Pouquet, Phys. Rev. E **74**, 016303 (2006).
[7] C. Cichowlas, P. Bonaïti, F. Debbasch, and M. E. Brachet, Phys. Rev. Lett. **95**, 264502 (2005).
[8] U. Frisch, B. Hasslacher and Y. Pomeau, Phys. Rev. Lett. **56**, 1505 (1986).
[9] S. Succi, P. Santangelo and R. Benzi, Phys. Rev. Lett. **60**, 2738 (1988).
[10] C. Nore, M. Abid, and M. E. Brachet, Phys. Rev. Lett. **78**, 3896 (1997).
[11] U. Frisch, S. Kurien, R. Pandit, W. Pauls, S. S. Ray, A. Wirth, and J. Z. Zhu, Phys. Rev. Lett. **101**, 144501 (2008).
[12] G. Krstulovic and M. E. Brachet, Physica D **237**, 2015 (2008).
[13] D. O. Gómez, P. D. Mininni, and P. Dmitruk, Phys. Scr. **T116**, 123 (2005); Adv. Space Res. **35**, 889 (2005).
[14] D. Gottlieb and S. A. Orszag, *Numerical Analysis of Spectral Methods: Theory and Applications* (SIAM, Philadelphia, 1977).
[15] S. A. Orszag, J. Fluid Mech. **41**, 363 (1970).
[16] The Liouville equation requires a statistical ensemble of initial data however, by ergodicity, the small scales of *a single* initial condition do statistically equilibrate.
[17] W. J. T. Bos and J.-P. Bertoglio, Phys. Fluids **18**, 071701 (2006).
[18] J. C. André and M. Lesieur, J. Fluid Mech. **81**, 187 (1977).
[19] J. Baerenzung, H. Politano, Y. Ponty, and A. Pouquet, Phys. Rev. E **77**, 046303 (2008).
[20] P. D. Mininni and A. Pouquet, Phys. Rev. E **79**, 026304 (2009); J. Baerenzung, P. D. Mininni, and A. Pouquet (unpublished).
[21] M. Lesieur and D. Schertzer, J. Mec. **17**, 609 (1978).